

High-power, high-efficiency continuous-wave Tm:KYW laser with multimode in-band diode pumping

Firas Trawi*, Marin Hamrouni, Zekican Ertürk, Lukas W. Perner , Valentin J. Wittwer, and Thomas Südmeyer

Laboratoire Temps-Fréquence (LTF), Institut de Physique, Université de Neuchâtel, Avenue de Bellevaux 51, 2000 Neuchâtel, Switzerland

Received 25 February 2026 / Accepted 19 April 2026

Abstract. We report a high-power, high-efficiency continuous-wave Tm:KY(WO₄)₂ (Tm:KYW) laser based on multimode in-band diode pumping at 1720 nm. In-band pumping reduces the quantum defect compared to conventional 800-nm pumping, enabling efficient high-power operation. We demonstrate up to 4.55 W of output power near 1.94 μm with a slope efficiency of 83% with respect to absorbed pump power, approaching the quantum-defect limit. The laser provides smooth wavelength tunability from 1839 to 2100 nm and maintains near-diffraction-limited transverse beam quality across the full operating range. These results indicate that multimode in-band pumping of Tm:KYW is a simple and compact route to efficient, broadband, high-power sources in the 1.9–2.0 μm region, providing a practical basis for future high-power Q-switched and mode-locked systems.

Keywords: Continuous-wave lasers, High-power lasers, In-band multimode diode pumping, Purged operation, CW Tm:KYW laser, SWIR lasers.

1 Introduction

Solid-state lasers offering high-power and tunable wavelengths in the 2-μm band are of considerable interest for many applications. When combined with diode pumping, these lasers are efficient, simple and cost-effective short-wavelength infrared (SWIR) sources. The 2-μm window is especially compelling as it overlaps strong H₂O rovibrational lines, enabling sensitive water-vapor spectroscopy and DIAL/LIDAR humidity profiling [1, 2], and it lies within an eye-safe atmospheric transmission band advantageous for free-space optical links and airborne sensing [3, 4]. It is also appealing for clinical applications such as endourology and soft-tissue surgery, where shallow optical penetration and efficient hemostasis are decisive [5, 6].

The most common gain media for high-power emission around 2 μm are based on Thulium (Tm), Holmium (Ho) and co-doped Tm/Ho ions. These three types of gain media feature different properties and their suitability depends on the application [7]. For instance, with a high emission cross-section around 2.1 μm and good thermal properties, Ho-doped crystals are ideal to deliver high average power beyond 2 μm [8]. However, these lasers are pumped around 1.9 μm and typically require a high-power single mode Tm-based laser as a primary pump source, increasing cost and

complexity of the overall setup. In contrast, Tm-doped crystals feature a strong absorption peak around 800 nm corresponding to the ³H₆ → ³H₄ transition of Tm³⁺ ions, which is conveniently accessed by high-power off-the-shelf and mature AlGaAs diode lasers. Co-doping with Tm and Ho ions has been developed for combining the convenient pumping of Tm around 800 nm and the strong emission of Ho near 2.1 μm. While these crystals have demonstrated excellent results for broadband emission [9], these materials are prone to enhanced up-conversion processes [10] compared with singly Tm-doped crystals, which increases the thermal load, reduces efficiency, and constrains power scaling. For these reasons, Tm-based gain media remain ideal candidates for applications requiring simple and compact high-power sources.

Tm-based lasers using multimode diode pumping around 800 nm have been demonstrated many times with a large variety of host materials [11–20]. Despite the large quantum defect associated with the ³H₆ → ³H₄ transition, this scheme relies on the cross-relaxation (CR) effect, known as a “two-for-one” energy-transfer process, which populates the upper laser level ³F₄, resulting in efficient laser operations [11, 17, 18, 20]. For instance, Ref. [17] reports on a 5-at.-%-doped Tm:KYW bulk laser demonstrating up to 73% of slope efficiency with respect to pump power, considerably larger than 41% expected from the quantum defect alone. Since the CR probability depends on the

* Corresponding author: fras.trawi@unine.ch

inter-ion spacing, it benefits from higher Tm^{3+} concentrations for efficient operation. Increasing doping concentration, however, also increases deleterious effects such as up-conversion, residual reabsorption, and concentration quenching, which can all play against high-power operation. Furthermore, the CR process generates additional heat due to the mismatch between the energy levels involved [21–24]. Although several efforts have aimed at further boosting efficiency at watt-level output powers, achieving such performance typically requires careful optimization and a more constrained resonator design. One effective approach is to use channel-waveguide laser geometries, which offer strong confinement and high pump absorption. For example, a channel-waveguide Tm laser [25] has demonstrated efficiencies as high as 80% at 1.6 W of average output power.

Alternatively, in-band pumping at 1.65–1.85 μm , which directly excites Tm^{3+} ions into the upper laser level manifold ${}^3\text{F}_4$, is highly promising for further increasing power and efficiency. The low quantum defect associated with in-band pumping substantially reduces thermal load due to non-radiative transitions and eliminates the dependence on Tm–Tm cross-relaxation for high efficiency. Furthermore, the absorption peak corresponding to in-band pumping is significantly broader than its counterpart at 800 nm, which makes it less sensitive to pump wavelength and temperature variations [26, 27]. In most cases, Raman-shifted Er-fiber or short-wavelength Tm-fiber lasers are employed to achieve in-band pumping. While such an approach has been successfully applied to different crystal hosts and demonstrated watt-level operation [26, 28, 29], the cost and complexity of the pump scheme is an obstacle for the adoption of the technology beyond laboratory settings. Recently, high-brightness pump diode sources around 1.7 μm have become commercially available, making in-band diode pumping a simple and cost-effective alternative. Although multimode in-band pumping for Tm-doped gain media has already led to high average power and efficiency, this approach remains scarce and has been demonstrated with only a few different hosts [30, 31].

In the family of promising monoclinic double-tungstate host materials, $\text{Tm:KY}(\text{WO}_4)_2$ (Tm:KYW) is particularly compelling. In addition to their commercial availability and robustness, Tm:KYW crystals have a large emission cross-section and broad gain bandwidth across ~ 1.9 – 2.1 μm , which make them ideal for operation at high power, broad wavelength tunability, and generation of short pulses [17, 27, 32]. Tm:KYW exhibits suitable broad absorption bands for in-band diode pumping around 1.7 μm , with pronounced peaks at 1678 nm and 1716 nm [27, 32]. Although the magnitude of the absorption peaks in Tm:KYW around 1.7 μm is reduced by about a factor of 2.5 compared to conventional 800-nm pumping, it is largely compensated by the availability of high-power multimode pump diodes, and the high quantum-limited efficiency of 80–90%. So far only one study reports on multimode diode in-band pumping with Tm:KYW [27], and the authors demonstrate only 86 mW of average output power with a moderate slope efficiency of 28%.

In this work, we employ multimode in-band pumping in a Tm:KYW laser oscillator and demonstrate high average

powers up to 4.55 W around 1940 nm with a slope efficiency of 83%; approaching the quantum-defect limit. To the best of our knowledge, this constitutes both the highest efficiency and average power, as compared to previous Tm:KYW-based bulk systems and, more generally, even among Tm-doped double-tungstate crystal bulk lasers. In addition, the source offers smooth wavelength tunability from 1839 to 2100 nm and maintains excellent, near-diffraction-limited beam quality across the full operating range.

This simple, cost-effective and single-stage source is promising for many applications requiring high-power levels and broad tunability and motivates Kerr-lens mode locking in a purged cavity to exploit the Tm:KYW broad gain bandwidth for high power and efficiency sub-100-fs pulse generation near the central gain.

2 Experimental setup

The experimental setup is shown in Figure 1a. The laser is based on a 3-mm-long Tm:KYW gain medium with 4.6 at.% doping, cut along the N_g . For thermal management, the crystal was wrapped in indium foil and mounted on a Peltier-cooled copper heatsink stabilized to around 12°C. Pumping is provided by a 15 W-rated fiber-coupled ($\text{NA} = 0.22$, 105 μm core diameter) diode laser at 1720 nm with roughly 10 nm FWHM spectral width. The pump light is unpolarized. Although the absorption around 1720 nm in the crystal is stronger for polarization along N_m than along N_p [27, 32], the high available pump power was sufficient to compensate for this difference. Therefore, for experimental convenience, no polarization-selection element is introduced in the pump scheme. N_p , N_m and N_g denote the principal axes of the dielectric frame of the monoclinic Tm:KYW crystal, where N_p is parallel to the crystallographic b-axis and N_m and N_g lie in the a–c plane. The diode is mounted on a water-cooled copper heat sink. To avoid crystal damage, we limit the incident pump power to 11.5 W. For experimental convenience, the absorbed pump fraction was measured in a temporary two-mirror resonator designed to reproduce the pump and laser mode sizes and intracavity power conditions of the final cavity, while allowing direct measurement of the transmitted pump. Under lasing operation, an absorbed-pump fraction of $(50 \pm 1)\%$ was obtained, consistent with reported values for in-band-pumped Tm:KYW [27, 29]. The pump scheme was single-pass. A pair of achromatic doublets (L1 and L2) with AR-AR coatings for the pump are used to image the fiber output into the crystal with a 1:1 ratio, producing a clean circular pump spot with a radius of 52.5 μm at the waist inside the crystal.

A Z-shaped hemispherical cavity with a total length of approximately 36 cm was implemented. The cavity directly starts with the entrance facet of the crystal. One facet of the Tm:KYW crystal carried a dichroic coating providing high pump transmission ($T \approx 96\%$ at 1.72 μm) while being highly reflective across the lasing range (HR, 1.85–2.1 μm). The second facet was AR-coated at both the pump and laser wavelengths. The crystal is followed by a concave mirror (CM, ROC -100 mm), and then a plane mirror. Both mirrors

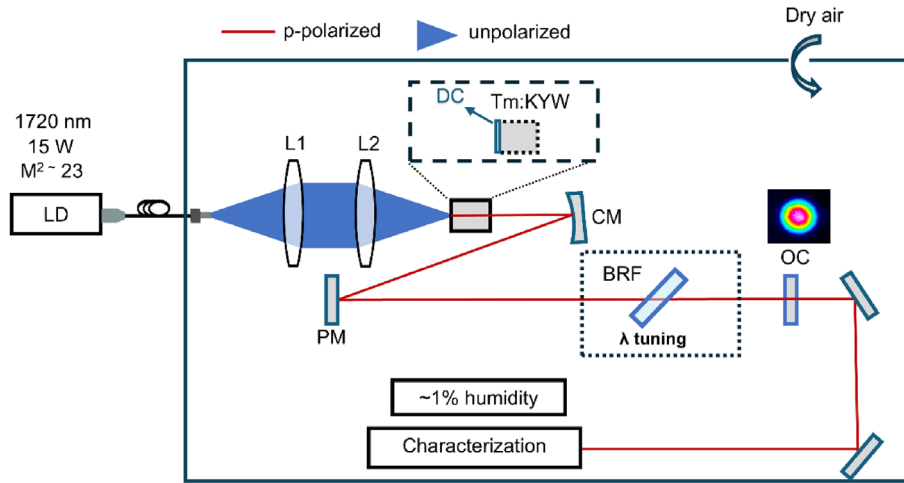


Figure 1. Schematic of the in-band-pumped Tm:KYW CW laser inside the dry-air-purged enclosure. LD – 1720 nm fiber-coupled laser diode; L1, L2 – AR-coated lenses imaging the fiber output into the crystal; Tm:KYW – 3-mm gain crystal with a dichroic coating (DC) that is anti-reflective (AR) for the pump and highly-reflective (HR) for the laser deposited on the facet towards the pump; CM – concave mirror (ROC –100 mm); PM – plane mirror; OC – plane output coupler; BRF – 2-mm-thick quartz birefringent filter used only for wavelength-tuning experiments (dashed box).

have a custom HR coating in the 1.85–2.1 μm range. The cavity is terminated with an output coupler (OC). To investigate laser performance over a wide operating range, we vary the output coupling rate from 0.6% to 7.5%. To study the wavelength tunability, an optional 2-mm-thick crystal-quartz birefringent filter (BRF) with its optical axis lying in the surface plane at Brewster's angle is introduced before the OC. This cavity leads to an estimated laser beam radius of 55 μm ($1/e^2$) in the crystal, based on a formalism of ray transfer matrices for Gaussian beam. The laser beam is polarized along the N_m axis, corresponding to p-polarization in our optical setup, in agreement with the Tm:KYW emission cross section, whose largest magnitude is along the N_m axis [27, 32].

The output power was measured with a calibrated thermopile power detector (Gentec UP19K-15S-H5). The transverse intensity profile was recorded using a DataRay WinCamD-FIR2 camera (pixel size $17 \times 17 \mu\text{m}^2$). The output spectrum was acquired with an APE WaveScan USB spectrometer (spectral resolution $< 0.5 \text{ nm}$).

The targeted application requires mode-hop-free tuning, hence the entire laser setup was enclosed in a sealed box continuously purged with dry air to drastically reduce water-vapor absorption in the Tm:KYW emission region. The relative humidity was monitored with a Thorlabs TSP01 sensor (accuracy $\pm 4\%$ below 20% humidity). We measure a residual relative humidity of 1% below the accuracy of the detector. All diagnostic devices were placed inside the purged enclosure to minimize the influence of water absorption on measured data.

3 Experimental results

Figure 2a shows the laser output power as a function of absorbed and incident pump power for the three OCs (0.6%, 2%, and 7.5%), in unpurged (dashed lines) and in

the purged configuration (solid lines). For all pump powers and output-coupler (OC) transmissions, we obtained stable CW operation of the Tm:KYW laser in the fundamental TEM_{00} mode.

The slope efficiency was extracted from a linear fit to the linear scaling region of the output laser power as a function of absorbed pump power. The lasing threshold was taken as the x-intercept of this fit. For the 7.5% output coupler, the power scaling remains essentially linear over the fully investigated pump range. For 0.6% and 2.0% output coupling, the scaling is also close to linear over most of the range, with only a slight roll-off appearing at the highest absorbed pump powers ($\geq 5 \text{ W}$), therefore, the linear fit was restricted to the range where the dependence remains linear. Overall, increasing the output coupling rate increases the extracted slope efficiency and yields higher output powers for a given pump power. With the 7.5% output coupler under purged operation, the laser delivers up to 4.55 W for 5.7 W of absorbed pump power, corresponding to an optical-to-optical efficiency of 80% (40%) with respect to absorbed (incident) pump power. The lasing threshold is reached at 0.16 W of absorbed pump power, corresponding to 0.31 W of incident pump power.

Compared to previously reported in-band-pumped CW Tm:KYW lasers, these values represent around 3.1-fold increase in output power and almost 33% higher slope efficiency than Ref. [29], where a 1750 nm Tm-fiber laser was used for pumping. Relative to Ref. [27], which employed a 1750 nm multimode diode pump, we see an increase in output power by a factor > 50 and an almost threefold improvement in slope efficiency. These results show the strong advantage of multimode high-power in-band pumping for achieving both high power and high efficiency operation with a simple and compact design.

For comparison, we also measured the power in unpurged operation (dashed lines), showing a few-percent

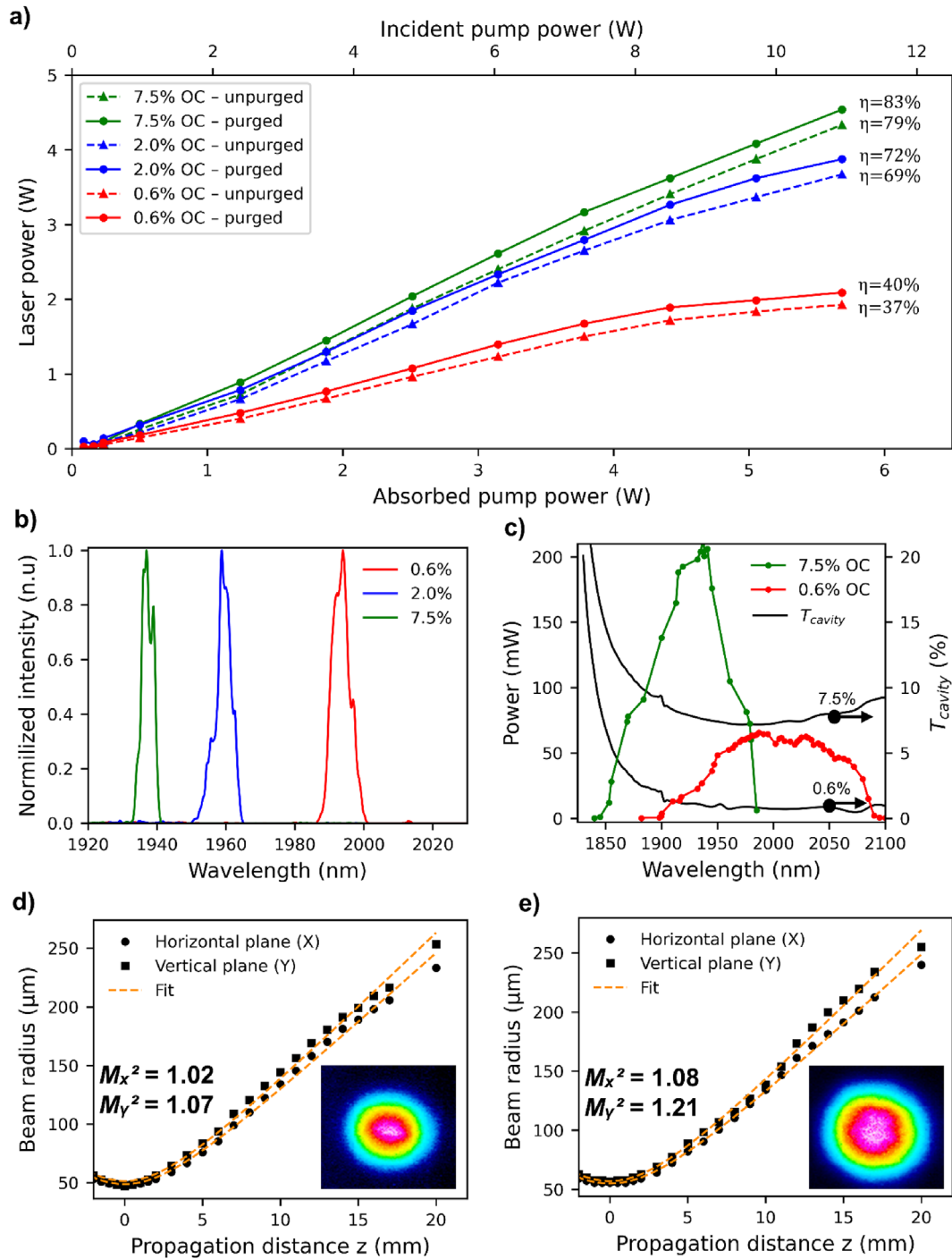


Figure 2. (a) Output power versus absorbed (bottom axis) and incident (top axis) pump power for three output couplers (OC = 0.6% in red, 2% in blue, 7.5% in green) in free air (dashed) and under dry-air purging (solid). The slope efficiencies with respect to absorbed pump power are indicated next to each curve. (b) Normalized laser spectra for the three OCs in the purged cavity. (c) Wavelength tuning with OC = 0.6% (red) and OC = 7.5% (green) at pump powers slightly above threshold for purged operation; the calculated total cavity transmission ($T_{cavity}(\%)$) for each configuration is shown in black (right axis). (d) Measurement results of the beam propagation parameter M^2 for low power operation $P_{\text{pump}} = 1$ W, yielding $P_{\text{laser}} = 0.26$ W with corresponding M^2 fits; the inset shows the transverse beam profile. (e) same as (d) but for high-power operation at $P_{\text{pump}} = 10$ W, yielding $P_{\text{laser}} = 3.9$ W.

decrease in output power and efficiency in all OC configurations when compared to dry-air operation. This is expected since the laser naturally operates where the overall gain is

the highest accommodating its CW spectrum between water absorption lines, and only a fraction of the generated spectrum is affected by water absorption.

Figure 2b shows the normalized CW spectra at output coupling rates of 0.6%, 2.0%, and 7.5% in dry-air operation. The laser emission shifts to shorter wavelengths as the output coupling increases, as is characteristic of quasi-three-level operation. We observe smooth and continuous spectra, confirming the effective suppression of water-vapor absorption.

Figure 2c shows the wavelength tuning measurements. On the left y -axis we show the output power with output coupling rate of 0.6 % (red) and output coupling rate of 7.5 % (green) at various wavelengths. The right y -axis shows the calculated overall cavity transmission for both configurations (grey curves). For each output coupler (OC), the incident pump power was kept constant over the entire tuning range and set slightly above the lasing threshold measured without the birefringent filter (BRF). Specifically, for the 0.6% OC, the incident pump power was fixed at 0.39 W (lasing threshold without BRF: 0.17 W), and for the 7.5% OC, it was fixed at 0.68 W (lasing threshold without BRF: 0.31 W). Operating near threshold reduces gain saturation and thermal load, so the tuning behavior is primarily governed by the crystal gain cross section rather than thermal effects, while maintaining sufficient margin to prevent the laser from switching off over the entire wavelength scan.

At an output coupling rate of 0.6% (red), a broad tuning range from around 1900 nm up to 2100 nm is obtained. The strongest output is observed in the 1980–2000 nm region. In the long-wavelength range, spectral tuning is limited to 2100 nm by the rapidly decreasing emission cross section [27, 32]. Below 1900 nm, spectral tuning is limited by the significant increase of cavity losses (grey solid line). At an output coupling rate of 7.5% (green), the tuning range shifts towards a shorter wavelength and becomes narrower, from 1840 nm to 1980 nm, with a peak around 1940 nm. The change and the shift of the overall spectral shape is mainly due to the higher inversion level, caused by the increased output coupling rate. Below 1850 nm, spectral tuning is limited by the significant increase of the cavity losses (grey solid line). Above 1980 nm, wavelength tuning is limited by the finite modulation depth of the BRF filter. In that region, the modulation depth of the filter is smaller compared to the difference between the peak and the tail of the gain cross-section [27, 32].

The transverse beam profile and beam-propagation factors are shown Figures 2d and 2e. The beam profiles were acquired with a DataRay WinCamD-FIR2 camera (pixel size $17 \times 17 \mu\text{m}^2$), while M^2 measurements were performed using a DataRay BeamMap2-DD slit scanning beam profiler. In low-power operation (Fig. 2d), at $P_{\text{pump}} = 1 \text{ W}$; $P_{\text{laser}} = 0.26 \text{ W}$, the estimated beam quality factors for the horizontal and vertical planes are $M_x^2 = 1.03$ and $M_y^2 = 1.08$. In high-power operation at $P_{\text{pump}} = 10 \text{ W}$, yielding $P_{\text{laser}} = 3.9 \text{ W}$, the estimated beam quality factors for both planes slightly increase to $M_x^2 = 1.08$ and $M_y^2 = 1.21$. The results confirm excellent beam quality with low astigmatism across the entire operation range, suggesting negligible thermal effects.

4 Conclusion

We have demonstrated multi-watt continuous-wave operation of a Tm:KYW laser in-band diode-pumped at $1.7 \mu\text{m}$ with a slope efficiency close to the quantum-defect limit in a dry-air purged environment. The laser delivers 4.55 W at $1.937 \mu\text{m}$ with an optical-to-optical slope efficiency of 83%. To our knowledge, this result demonstrates the highest power and efficiency achieved by any CW in-band-pumped Tm:KYW laser and even among Tm-doped double-tungstate crystal bulk systems. The laser is tunable from 1839 to 2100 nm and maintains excellent beam quality over the full power range, while maintaining a simple Z-shaped cavity and using a basic multimode pump diode. Further optimization and miniaturization may be possible by employing shorter and more highly doped Tm:KYW crystals, if supported by available crystal-growth methods and while preserving sufficient material quality, pump absorption, and crystal gain. This could help preserve the high pump absorption and crystal gain while improving the pump–laser mode overlap in the crystal. Efficient operation of 8 at. % [33] and 15 at. % [34] Tm-doped double tungstate lasers was already demonstrated in a waveguide and thin-disk geometry respectively. As a key message, this work shows that in-band pumping around 1700 nm based on a multimode diode, which became commercially available recently, is a simple and cost-effective effective solution for efficient high-power operation near $2 \mu\text{m}$. Also, we believe that this platform will open a new route toward the development of powerful 2- μm mode-locked lasers.

Funding

Schweizerischer Nationalfonds zur Förderung der Wissenschaftlichen Forschung (10002591, 219395, 198176).

Conflicts of interest

The authors declare that they have no competing interests.

Data availability statement

Data underlying this paper can be obtained from the authors upon reasonable request.

Author contribution statement

F.T. and Z.E. performed the experimental work with assistance of M.H., V.J.W. and L.W.P. F.T. and M.H. analyzed the data and wrote the manuscript. T.S. supervised the project.

References

1. Carroll BJ, Nehrir AR, Kooi SA, Collins JE, Barton-Grimley RA, Notari A, Harper DB, Lee J, Differential absorption Lidar measurements of water vapor by the High Altitude Lidar Observatory (HALO): retrieval framework and first results, *Atmos. Meas. Tech.* **15**(3), 605–626 (2022). <https://doi.org/10.5194/amt-15-605-2022>.

2. Endemann M, Byer RL, Simultaneous remote measurements of atmospheric temperature and humidity using a continuously tunable IR lidar, *Appl. Opt.*, **20**, 18, 3211–3217 (1981). <https://doi.org/10.1364/AO.20.003211>.
3. Lin P, Wang T, Ma W, Chen J, Jiang Z, Yu C, 2- μm free-space data transmission based on an actively mode-locked holmium-doped fiber laser, *IEEE Photonics Technol. Lett.* **32**(5), 223–226 (2020). <https://doi.org/10.1109/LPT.2020.2968073>.
4. Siegel T, Chen S-P, Investigations of free space optical communications under real-world atmospheric conditions, *Wireless Pers. Commun.* **116**(1), 475–490 (2021). <https://doi.org/10.1007/s11277-020-07724-1>.
5. Fried NM, Murray KE, High-power thulium fiber laser ablation of urinary tissues at 1.94 μm , *J. Endourol.* **19**(1), 25–31 (2005). <https://doi.org/10.1089/end.2005.19.25>.
6. Hou S-P, Wang Y-G, Application status of holmium and thulium fiber laser for urological calculi, *Front. Phys.* **13** (2025). <https://doi.org/10.3389/fphy.2025.1590456>.
7. Walsh BM, Review of Tm and Ho materials; spectroscopy and lasers. *Laser Phys.* **19**, 855–866 (2009). <https://doi.org/10.1134/S1054660X09040446>.
8. Yao W, Wang Y, Tomilov S, Hoffmann M, Ahmed S, Liebold C, Rytz D, Peltz M, Wesemann V, Saraceno CJ, 8.7-W average power, in-band pumped femtosecond Ho:CALGO laser at 2.1 μm , *Opt. Express, OE* **30**(23), 41075–41083 (2022). <https://doi.org/10.1364/OE.471341>.
9. Yuan J, Wang W, Ye Y, Deng T, Huang Y, Gu S, Chen Y, Xiao P, 2.0 μm Ultra broadband emission from Tm³⁺/Ho³⁺ Co-Doped gallium tellurite glasses for broadband light sources and tunable fiber lasers, *Crystals* **11**(2), 190 (2021). <https://doi.org/10.3390/cryst11020190>.
10. Lagatsky AA, Fusari F, Kurilchik SV, Kisel VE, Yasukevich AS, Kuleshov NV, Pavlyuk AA, Brown CTA, Sibbett W, Optical spectroscopy and efficient continuous-wave operation near 2 μm for a Tm, Ho:KYW laser crystal, *Appl. Phys. B* **97**(2), 321–326 (2009). <https://doi.org/10.1007/s00340-009-3698-2>.
11. Gaponenko M, Kuleshov N, Südmeyer T, Efficient diode-pumped Tm:KYW 1.9- μm microchip laser with 1 W cw output power, *Opt. Exp.* **22**(10), 11578–11582 (2014). <https://doi.org/10.1364/OE.22.011578>.
12. Demirbas U, Thesinga J, Beyatli E, Kellert M, Pergament M, Kärtner FX, Continuous-wave Tm:YLF laser with ultrabroad tuning (1772–2145 nm). *Opt Express, OE* **30**(23), 41219–41239 (2022). <https://doi.org/10.1364/OE.471288>.
13. Cemy P, Burns D, Modeling and experimental investigation of a diode-pumped Tm:YAlO/sub 3/ laser with a- and b-cut crystal orientations, *IEEE J. Selected Top. Quantum Electr.* **11**(3), 674–681 (2005). <https://doi.org/10.1109/JSTQE.2005.850239>.
14. Na Q, Xu C, Chen H, Yin J, Wang J, Yu Y, Yang J, Wang L, Yan P, Ruan S, Continuous-wave and mode-locking operation of Tm:YAP lasers near 1.8 μm , *Opt. Laser Technol.* **142**, 107225 (2021). <https://doi.org/10.1016/j.optlastec.2021.107225>.
15. Wang Y, Wang S, Wang J, Zhang Z, Zhang Z, Liu R, Zu Y, Liu J, Su L, High-efficiency ~ 2 μm CW laser operation of LD-pumped Tm³⁺:CaF₂ single-crystal fibers. *Opt Express, OE* **28**(5), 6684–6695 (2020). <https://doi.org/10.1364/OE.386659>.
16. Ryba-Romanowski W, Lisiecki R, Jelinková H, Šulc J, Thulium-doped vanadate crystals: growth, spectroscopy and laser performance, *Prog. Quant. Electr.* **35**(5), 109–157 (2011). <https://doi.org/10.1016/j.pquantelec.2011.06.001>.
17. Lagatsky AA, Calvez S, Gupta JA, Kisel VE, Kuleshov NV, Brown CTA, Dawson MD, Sibbett W, Broadly tunable femtosecond mode-locking in a Tm:KYW laser near 2 μm , *Opt. Express* **19**(10), 9995–10000 (2011). <https://doi.org/10.1364/OE.19.009995>.
18. Gao WL, Ma J, Xie GQ, Zhang J, Luo DW, Yang H, Tang DY, Ma J, Yuan P, Qian LJ, Highly efficient 2 μm Tm:YAG ceramic laser, *Opt. Lett., OL* **37**(6), 1076–1078 (2012). <https://doi.org/10.1364/OL.37.001076>.
19. Qin ZP, Liu JG, Xie GQ, Ma J, Gao WL, Qian LJ, Yuan P, Xu XD, Xu J, Zhou DH, Spectroscopic characteristics and laser performance of Tm:CaYAlO₄ crystal, *Laser Phys.* **23**(10), 105806 (2013). <https://doi.org/10.1016/j.optmat.2023.13610>.
20. Mateos X, Liu J, Griebner U, Petrov V, Pujol MC, Aguilo M, Diaz F, Galan M, Viera G, *Efficient continuous-wave laser operation of Tm:KLu(WO₄)₂ near 2 μm , in 2006 Conference on Lasers and Electro-Optics and 2006 Quantum Electronics and Laser Science Conference, (May 2006), paper 1–2.*
21. Khamis MA, Ennsner K, Theoretical model of a thulium-doped fiber amplifier pumped at 1570 nm and 793 nm in the presence of cross relaxation, *J. Lightwave Technol.* **34**(24), 5675–5681 (2016). <https://doi.org/10.1109/JLT.2016.2631635>.
22. Jackson SD, Cross relaxation and energy transfer upconversion processes relevant to the functioning of 2 μm Tm³⁺-doped silica fibre lasers, *Opt. Commun.* **230**(1), 197–203 (2004). <https://doi.org/10.1016/j.optcom.2003.11.045>.
23. Jackson SD, Mossman S, Efficiency dependence on the Tm³⁺ and Al³⁺ concentrations for Tm³⁺-doped silica double-clad fiber lasers, *Appl. Opt. AO* **42**(15), 2702–2707 (2003). <https://doi.org/10.1364/ao.42.002702>.
24. Buryy OA, Sugak DY, Ubizskii SB, Izhnin II, Vakiv MM, Solskii IM, The comparative analysis and optimization of the free-running Tm³⁺:YAP and Tm³⁺:YAG microlasers, *Appl. Phys. B* **88**(3), 433–442 (2007). <https://doi.org/10.1007/s00340-007-2718-3>.
25. van Dalßen K, Aravazhi S, Grivas C, García-Blanco SM, Pollnau M, Thulium channel waveguide laser with 1.6 W of output power and $\sim 80\%$ slope efficiency, *Opt. Lett. OL* **39**(15), 4380–4383 (2014). <https://doi.org/10.1364/OL.39.004380>.
26. Loiko P, Thouroude R, Soulard R, Guillemot L, Brasse G, Guichardaz B, Braud A, Hideur A, Laroche M, Gilles H, Camy P, In-band pumping of Tm:LiYF₄ channel waveguide: a power scaling strategy for ~ 2 μm waveguide lasers, *Opt. Lett. OL* **44**(12), 3010–3013 (2019). <https://doi.org/10.1364/OL.44.003010>.
27. Troshin AE, Kisel VE, Yasukevich AS, Kuleshov NV, Pavlyuk AA, Dumina EB, Kornienko AA, Spectroscopy and laser properties of Tm³⁺:KY(WO₄)₂ crystal, *Appl. Phys. B* **86**(2), 287–292 (2007). <https://doi.org/10.1007/s00340-006-2448-y>.
28. Yao W, Wu F, Zhao Y, Chen H, Xu X, Shen D, Highly efficient Tm:CaYAlO₄ laser in-band pumped by a Raman fiber laser at 1.7 μm , *Appl. Opt. AO* **55**(14), 3730–3733 (2016). <https://doi.org/10.1364/AO.55.003730>.
29. Tokurakawa M, Daniel JMO, Clarkson WA, Tm³⁺:KY(WO₄)₂ laser in-band pumped by a Tm fiber laser, in *Advanced Solid State Lasers, OSA Technical Digest (Online)* Optica Publishing Group, (2014), paper ATu2A.30. <https://doi.org/10.1364/ASSL.2014.ATu2A.30>.

30. Kratochvíl J, Šulc J, Jelínková H, Efficient 1.7 μm pumping of 2 μm thulium lasers, *Opt. Lett.* **48**(16), 4185 (2023). <https://doi.org/10.1364/OL.495369>.
31. Kratochvíl J, Veselský K, Popelová D, Šulc J, Jelínková H, Nejezchleb K, Uxa Š, Resonantly diode-pumped Tm:YAG laser for efficient 2036 nm generation, *Appl. Phys. B* **131**(3), 61 (2025). <https://doi.org/10.1007/s00340-025-08407-0>.
32. Guretskii SA, Trukhanova EL, Kravtsov AV, Gusakova NV, Gorbachenya KN, Kisel VE, Yasukevich AS, Lisiecki R, Lukowiak A, Karpinsky DV, Ozen Y, Ozcelik S, Kuleshov NV, *Tm³⁺:KY(WO₄)₂ single crystals: Controlled growth and spectroscopic assessment*, **111451** (2021). <https://doi.org/10.1016/j.optmat.2021.111451>.
33. van Daltsen K, Aravazhi S, Grivas C, García-Blanco SM, Pollnau M, Thulium channel waveguide laser in a monoclinic double tungstate with 70% slope efficiency, *Opt. Lett., OL* **37**(5), 887–889 (2012). <https://doi.org/10.1364/OL.37.000887>.
34. Vatnik S, Vedin I, Segura M, Mateos X, Pujol MC, Carvajal JJ, Aguiló M, Díaz F, Petrov V, Griebner U, Efficient thin-disk Tm-laser operation based on Tm:KLu(WO₄)₂/KLu(WO₄)₂ epitaxies, *Opt. Lett., OL* **37**(3), 356–358 (2012). <https://doi.org/10.1364/OL.37.000356>.